Microarticle

Collision-induced luminescence spectra of pyridine bombarded by 1000 eV He$^+$ cations

Tomasz J. Wasowicz

Department of Physics of Electronic Phenomena, Gdańsk University of Technology, ul. G. Narutowicza 11/12, 80-233 Gdańsk, Poland

ARTICLE INFO

ABSTRACT

Here we show collision-induced luminescence spectra measured for collisions of the He$^+$ cations with the aromatic six-membered ring of the pyridine molecule (C_5H_5N). Distinct emission bands due to the CH($A^2\Delta \to X^2\Pi_r$; $B^2\Sigma^+ \to X^2\Pi_r$; $C^2\Sigma^+ \to X^2\Pi_r$), CN($B^2\Sigma^+ \to X^2\Sigma^+$), C_2($d^3\Pi_g \to a^3\Pi_u$), and NH($A^3\Pi \to X^3\Sigma^-$) transitions, as well as atomic H, He, and C lines have been observed. Apart from the He atoms, all the emitters arise from the fragmentation of the pyridine ring. The identification of the helium lines indicates a single electron transfer reaction from the pyridine molecule to the He$^+$ cations. The products' intensities relative to the H$_\beta$ intensity have also been obtained and compared with the intensity ratios determined for He$^+$ + furan collisions.

Introduction

The knowledge of dissociation processes of chemical compounds into smaller molecules, atoms, ions, or radicals constitutes an essential issue in modern science. Chemical reactions occurring naturally and used in engineering ensue by forming some bonds and rupturing other ones. A molecule dissociation may be initiated by radiation propagating from a source as an electromagnetic wave or a beam of the particles. The charged dissociation products can be directly investigated using mass spectrometric techniques, whereas dissociation into neutral fragments is more challenging to study experimentally. However, when the fragments are formed in the excited states, then they can be probed by the detection of their emission. While the fluorescence spectroscopy has been widely used in the analysis of neutral products in the studies of the photon and electron interactions with matter (see, e.g. [1–4], and references therein), the ion-induced neutral dissociation of molecules has not been as extensively explored. In recent years, the attention has mostly been paid to investigate the collisional mechanisms via the analysis of the luminescence spectra of simple molecules [5–9]. However, to the best of our knowledge, only our group and that of Mayer's have reported researches probing the ion-induced neutral dissociation of larger polyatomic targets [10–15].

Since heterocyclic molecules containing N and O atoms play a significant role in many fields of biology, chemistry, and medicine, ranging from organic synthesis to molecular genetics, these compounds are of particular interest to our group. Therefore, here we show the results of the fragmentation into neutral fragments of the gas-phase pyridine, a model heterocyclic molecule, in collisions with 1000 eV He$^+$ cations.

Helium was selected because, on the one hand, it is the second most common element in the universe [16], and on the other hand, its possible clinical implementations in hadron therapies are nowadays considered [17]. Thus He$^+$ cations seem to be the ideal candidates as the model objects in the studies of the ion-neutral molecule interactions occurring in these environments. The aromatic six-membered ring of the pyridine molecule, C_5H_5N, comprises one nitrogen atom that substitutes the CH group in benzene, and for that purpose, pyridine is one of the simplest nitrogen-containing heteroaromatic compounds. It is of high importance to studies of fragmentation processes because it exhibits a wide spectrum of targets and broad biological [18], chemical [19], and astrophysical [20] activities. However, the literature on the ion-induced fragmentation of the gas phase pyridine is very scarce. Excluding our report on the hydrogen atom migration preceding dissociation of the pyridine molecules by the H$^+$, H$_2{}^+$, He$^+$, He^{2+}, and O$^+$ impact [10], the insight into the pyridine fragmentation was only shed by low energy (10 to 22 eV) studies of rate coefficients for several ionic projectiles performed by Fondren *et al.* [21]. Thus in this study, we have utilized the collision-induced emission spectroscopy to explore the collisional excitation products and the spectral signatures of collisional mechanisms occurring in the He$^+$ + C_5H_5N impact system.

Experiment

The experiments were performed at the University of Gdansk using collision-induced emission spectroscopy (CIES) described in detail in [6,11]. The newest drawing of the appliance and methodology of measuring were described in [10,12,13]. The experimental conditions
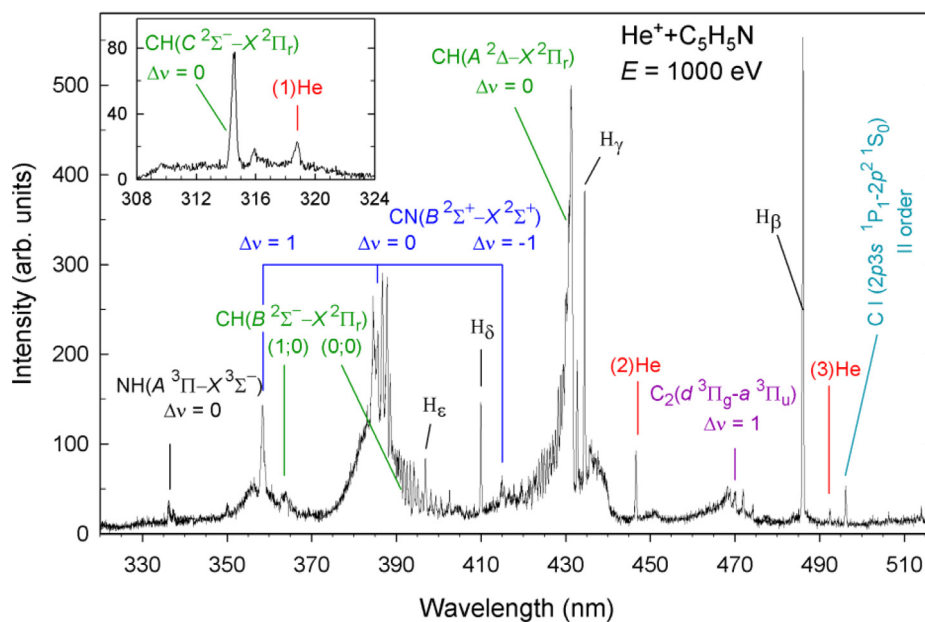
Fig. 1. Collision-induced luminescence spectra measured with an optical resolution $\Delta\lambda$ of 0.4 nm for collisions of the pyridine molecules with He$^+$ cations. The spectra were not corrected for the wavelength dependence of the sensitivity of the detection system.

and the settings utilized in the experiment are presented in Experimental details of Supplemental information. In brief, the apparatus consisted of four parts: an ion source, a mass selector, a collision chamber, and an optical spectrometer. The ions were generated from the helium gas utilizing the Colutron hot cathode discharge. Then, they were directed into a 60° magnetic mass selector, which separated them according to the m/q ratio. In the collision cell, the ions impinged upon the vapors of the target molecules leading to their fragmentation. The emission of the products generated in the excited states was detected with a sensitive multi-channel photon detector mounted in the optical spectrometer. The spectrometer operated on two gratings. The 1200 lines/mm grating allowed us to measure the high-resolution collision-induced luminescence spectra $\Delta\lambda$ of 0.4 nm (FWHM), which were appropriate for the accurate identification of the spectral components. The second grating, 300 lines/mm, was used to measure luminescence spectra in the 180–540 nm wavelength range and obtain the relative intensities of the emission lines.

Results and discussion

Fig. 1 presents the luminescence spectra measured in the 300–520 nm wavelength for the He$^+$ + C$_5$H$_5$N collisions. As expected, the dominant luminescence signals detected correspond to atomic and diatomic fragments arising from the fragmentation of the excited pyridine molecule. Indeed, similar emission spectra were observed by us in the photodissociation of pyridine [22], as well as in our previous related cation-induced experiments [10]. Also, the most recent emission spectra from collisions of 8 keV He$^+$ and H$_2^+$ cations with benzene and naphthalene molecules revealed hydrocarbon skeleton fragmentation into the atomic and diatomic species [15]. We identified the emission features of molecular fragments by comparing our luminescence spectra with the fluorescence spectra obtained by us previously and by other authors in, for example, laser-induced fluorescence investigations [10,22–28]. The positions and assignments of the atomic lines were found using information from the NIST Atomic Spectra Database [29]. The emissions observed in the He$^+$ collisions with pyridine, their estimated threshold energies, and positions are listed in Table S1 of Supplemental information.

The major emission comes from the vibrationally and rotationally excited CH radicals. The CH fragments were created with excitation to

the A$^2\Delta$, B$^2\Sigma^+$, and C$^2\Sigma^+$ electronic states (see Fig. S1 of Supplemental information) that decay via transitions to the X$^2\Pi_r$ state. The shape of the strongest A$^2\Delta \to$ X$^2\Pi_r$ emission band of the CH fragment (shown in detail in Fig. S2 of Supplemental information) arises from the overlapping rotational lines of the (0,0), (1,1) and (2,2) vibrational transitions [23,24]. The second CH band, B$^2\Sigma^+ \to$ X$^2\Pi_r$, consists of the rotational lines of the (0,0) and (1,0) vibrational transitions [23,24]: the (0,0) rovibrational lines spread over the wavelength range of 386.5–409.0 nm while the (1,0) band appears at the 362.5–368.5 nm. The emission band of the CH(C$^2\Sigma^+ \to$ X$^2\Pi_r$) appears in the 308–324 nm region [23]. The pattern of this band is less intense than the other two and contains the overlying rotational lines of the (0,0) and (1,1) vibrational transitions [23]. The 349–390 nm spectral region exhibits quite intense luminescence of the B$^2\Sigma^+ \to$ X$^2\Sigma^+$ rovibrational bands of the CN molecule [22]. Its $\Delta\nu = 0$ and $\Delta\nu = 1$ bands appear in the 373–389 and 351–359 nm regions, respectively [22]. Sharp peaks at 388.5, 387.4, and 386.4 nm belong to the band heads of the P branches of the (0,0), (1,1), and (2,2) transitions, respectively [22,25]. The (1,1) vibrational band of the CN overlaps with the band head of the R branch of the (0,0) transition of CH(B$^2\Sigma^+ \to$ X$^2\Pi_r$) [25]. Moreover, in the 415–420 nm range the B$^2\Sigma^+ \to$ X$^2\Sigma^+$ bands ($\Delta\nu = -1$) of the excited CN lay over the low wavelength shoulder of CH(A$^2\Delta \to$ X$^2\Pi_r$) (see Fig. 1). The d$^3\Pi_g \to$ a$^3\Pi_u$ Swan system of the excited C$_2$ fragments covers the spectral region from 445 to 480 nm. Well-resolved lines of the $\Delta\nu = +1$ vibrational sequence consisting of the band heads (1,0) at 473.7 nm, (2,1) at 471.5 nm, (3,2) at 469.7 nm, (4,3) at 468.4 nm, and (5,4) at 467.8 nm can be recognized in Fig. 1 [26]. Apart from the molecules mentioned, the NH radicals are identified by detection of the A$^3\Pi \to$ X$^3\Sigma^-$ emission, which emerges from 326 nm up to 345 nm [10,27,28]. Since the skeleton of the pyridine molecule consists of five CH units and one N heteroatom and has not got the NH structural entities, the appearance of the luminescence from the excited NH(A$^3\Pi$) is visible evidence of a chemical bond rearrangement process in which one of the hydrogen atoms migrates prior to the dissociation. This phenomenon has recently been investigated by us in the collisions of pyridine molecules with the H$^+$, H$_2^+$, He$^+$, He^{2+}, and O$^+$ cations applying the CIES [10] as well as in the photodissociation of pyridine [27]. In particular, the cation-induced studies showed [10] that the physicochemical conditions necessary for the formation of the NH(A$^3\Pi$) depended on the mass and charge of the projectiles. Moreover, the

rearrangement of the pyridine molecule was selectively activated by tuning the impact energy [10]. The *ab initio* quantum chemical calculations suggested site-selective hydrogen migration from C(2) to N, accompanied by N–C(6) single bond rupture leading to the geometrically stable nonplanar open-ring pyridine isomer with a terminal NH group that can be released by the C(2) = N double-bound cleavage [27]. It is of note that the production of the NH($A^3\Pi$) free radicals was also observed and discussed in detail in the studies of smaller heterocyclic molecules, e.g., isoxazole [28] suggesting the importance of this fragmentation channel. The spectra of Fig. 1 display strong H$_\beta$ through to H$_\epsilon$ emission lines of the Balmer series, which identify dissociation of the pyridine molecules into the excited hydrogen H(n) atoms, $n = 4$–7. The noteworthy feature displayed in Fig. 1 is the occurrence of the emission from carbon atoms excited to the 2p3s $^1P_1$, which points to complex fragmentation of the pyridine ring. Indeed, these reactions can be related to the re-distribution of energy and rearrangement of its atoms. In particular disintegration of pyridine may start from an opening of the pyridyne ring by the scission of the weakest N–C(6) bond, accompanied by isomerization, followed by the C(5)=C(6) double-bound cleavage [22]. Then abstraction of two hydrogens releases the C atom [22]. Finally, in Fig. 1 the (1)He, (2)He, and (3)He lines at 318.8, 447.1, and 492.2 nm correspond to the atomic helium transitions (1s4p $^3P_0$-1s2s $^3S_1$), (1s4d ^3D-1s2p ^3P), and (1s4d $^1D_2$-1s2p $^1P_1°$), respectively. The pyridine ring lacks the helium atoms. Therefore observation of the emission lines of He is direct evidence of an impact reaction occurring via relocation of the electronic charge between the interacting entities, i.e., single electron transfer from target molecules to projectiles before the fragmentation.

Because we have recently investigated collisions of the He$^+$ with furan [13], which is one of the simplest building blocks of the oxygen-containing polycyclic aromatic hydrocarbons, in the next step, the results of both experiments were compared. Since the apparatus used did not enable us to perform measurements of the absolute emission cross-sections, which are the most suitable for such an examination, we compared the corresponding intensity ratios determined in both impact systems. For this purpose, each spectrum measured with the use of the 300 lines/mm grating was corrected for the wavelength dependence of the sensitivity of the optical system. Then, the intensities of the emission lines were obtained by integrating over the peak/band areas and normalizing to the incident ion beam current, acquisition time, and pressure. Next, the intensity ratios (listed in Table 1) were calculated as quotients of H$_\beta$ normalized intensity ($I_{H\beta}$) to the other product intensities (I_M). The compared ratios show that in the He$^+$ + C$_5$H$_5$N collisions, there is relative to H$_\beta$ more severe production of all the species apart from the CH($A^2\Delta$) radical. The fittings to the CH($A^2\Delta \to$ X$^2\Pi_r$) emission band (see Fig. S2 of Supplemental information) show, however, that this radical is formed with higher vibrational and rotational excitation. The He$^+$ + furan interactions yielded the CH products characterized by T_{vib} and T_{rot} temperatures lower of about 1500

and 500 K than the corresponding temperatures obtained in the present experiment. Even the electron transfer reaction seems to be more probable from pyridine than from furan. This likely results from the electronic structure of both molecules and projectiles (see Fig. S3 of Supplemental information). Resonant electron capture from the pyridine to He$^+$ cations is not energetically favored because the accessible state of projectile lies about 15 eV below the pyridine ionization potential. The situation in the He$^+$ + furan is more complicated because the energy difference is 0.66 eV higher than in the He$^+$ + pyridine. In the He$^+$ collisions with pyridine, less energy is thus required for charge transfer reaction suggesting that the production of excited helium atoms is here likely pronounced. Thus the comparison indicates different physical conditions occurring during both collisions and represents a quite sensitive tool that may be used to differentiate between various impact systems.

Summary

The collisional excitation products and the spectral signatures of collisional mechanisms occurring in the He$^+$ + C$_5$H$_5$N impact system have been identified and compared with the results of the He$^+$ + C$_4$H$_4$O collisions. Although in both collisional systems the luminescence spectra display a common set of excited atomic and diatomic products, some differences can be recognized. Indeed, the comparison shows the spectral signatures of specific fragments (i.e., CN, NH) only arising from pyridine fragmentation. The intensity ratios of all the compared products are different. While the experiments have been performed in very similar conditions with the use of the same projectiles, the He$^+$ + C$_5$H$_5$N collisions yielded vibrationally and rotationally "hotter" CH($A^2\Delta$) radicals than collisions with furan.

It is of note that in both impact systems, the act of collision could have triggered the dissociative excitation or ionization of the target molecule, electron transfer from the target to the He$^+$, the transient cation-molecule complex formation before fragmentation [10,13]. These reactions compete with each other, and it is challenging to recognize in such kinds of experiments which impact mechanism governs the fragmentation. However, the observation of the emission lines of He indicates that an impact reaction occurring via single electron transfer from target molecules to projectiles without a doubt occurred even if it was not a major impact mechanism. A full picture of collisional processes arising at the molecular level can only be elucidated in conjunction with the theory, and therefore the quantum chemical calculations of He$^+$ + C$_5$H$_5$N would be required.

CRediT authorship contribution statement

Tomasz J. Wasowicz: Conceptualization, Methodology, Formal analysis, Investigation, Writing - original draft, Visualization, Project administration, Funding acquisition.

Declaration of Competing Interest

The authors declare that they have no known competing financial interests or personal relationships that could have appeared to influence the work reported in this paper.

Acknowledgments

Table 1

Comparison of the intensity ratios obtained for He$^+$ collisions with pyridine and furan [13], respectively.

M	$I_{H\beta}/I_M$ at 1000 eV	
	He$^+$ + C$_5$H$_5$N	He$^+$ + C$_4$H$_4$O
H$_\gamma$	1.4 (0.1)	3.9 (0.8)
H$_\delta$	2.5 (0.2)	6.1 (0.8)
(2)He$_{\lambda = 447.1\ nm}$	3.2 (0.3)	5.1 (0.5)
C$_2$($\Delta v = 0, 1$)	0.38 (0.03)	0.58 (0.09)
CH($A^2\Delta$)	0.18 (0.01)	0.10 (0.01)
CH($B^2\Sigma^+$) + CN($B^2\Sigma^+$)	0.15 (0.01)	
CH($C^2\Sigma^-$)	2.2 (0.2)	
NH($A^3\Pi$)	5.1 (0.7)	
C$_{\lambda = 247.9\ nm}$	5.6 (0.5)	
C$_{\lambda = 193.1\ nm}$	2.1 (0.2)	

Appendix A. Supplementary data

Supplementary data to this article can be found online at https://doi.org/10.1016/j.rinp.2020.103244.

References

[1] McConkey JW, et al. Phys Rep 2008;466:1–103.
[2] Hatano Y. Phys Rep 1999;313:109–69.
[3] Wasowicz TJ, et al. Phys Rev A 2011;83:033411.
[4] Linert I, et al. Chem Phys Lett 2010;498:27–31.
[5] Donohue DE, et al. J Chem Phys 1977;67:769.
[6] Ehbrecht A, et al. Chem Phys Lett 1998;284:205–13.
[7] Poon C, Mayer PM. J Phys Chem A 2007;111:777–82.
[8] Pranszke B. Chem Phys Lett 2009;484:24–7.
[9] Drozdowski R, Kowalski A. Eur Phys J D 2018;72:220.
[10] Wasowicz TJ, Pranszke B. J Phys Chem A 2016;120:964–71.
[11] Wasowicz TJ, Pranszke B. Eur Phys J D 2016;70:175.
[12] Wasowicz TJ, Pranszke B. J Phys Chem A 2015;119:581–9.
[13] Wasowicz TJ, et al. Int J Mol Sci 2019;20:6022.
[14] Holmes JL, Mayer PM. Eur Mass Spectrom 1995;1:23–31.
[15] Rashid S, et al. Chem Phys Lett 2017;667:129–36.
[16] Zeitlin C, et al. Science 2013;340:1080–4.
[17] Tommasino F, et al. Int J Particle Ther 2015;2:428–38.
[18] Baumann M, Baxendale IR. Beilstein J Org Chem 2013;9:2265.
[19] Zhai Y-E, Shi D-Q. J Heterocycl Chem 2013;50:1039.
[20] Parker DSN, et al. Phys Chem Chem Phys 2015;17:32000–8.
[21] Fondren LD, et al. Int J Mass Spectrom 2007;265:60–7.
[22] Wasowicz TJ, et al. J Phys B: At Mol Opt Phys 2014;47:055103.
[23] Bass AM, Broida HP. A spectrophotometric atlas of the spectrum of CH from 3000 A to 5000 Å. U.S. Department of Commerce, National Bureau of Standards Monograph 24; 1961.
[24] Wasowicz TJ, et al. J Phys B: At Mol Opt Phys 2012;45:205103.
[25] Maksyutenko P. Rev Sci Instrum 2011;82:083107.
[26] Yadav D, et al. Spectrochim Acta, Part B 2009;64:986–92.
[27] Wasowicz TJ, et al. J Phys B: At Mol Opt Phys 2017;50:015101.
[28] Zubek M, et al. J Chem Phys 2014;141:064301.
[29] Kramida A, Ralchenko Yu, Reader J, NIST ASD Team. NIST Atomic Spectra Database (ver. 5.7.1), [Online]. Available: https://physics.nist.gov/asd [2020, April 14]. National Institute of Standards and Technology, Gaithersburg, MD; 2019. DOI: https://doi.org/10.18434/T4W30F.